Solubility, complexation and thermodynamics of the Tc(IV)–isosaccharinic acid system: Trends in the M(IV) series

Kyungwon Kim [a], Sarah B. Duckworth [b], Marcus Altmaier [b], Wooyong Um [a,c,d,*], Xavier Gaona [b,**]

[a] Pohang University of Science and Technology, Division of Advanced Nuclear Engineering, Pohang, 37673, Republic of Korea
[b] Karlsruhe Institute of Technology, Institute for Nuclear Waste Disposal, Eggenstein-Leopoldshafen, 76344, Germany
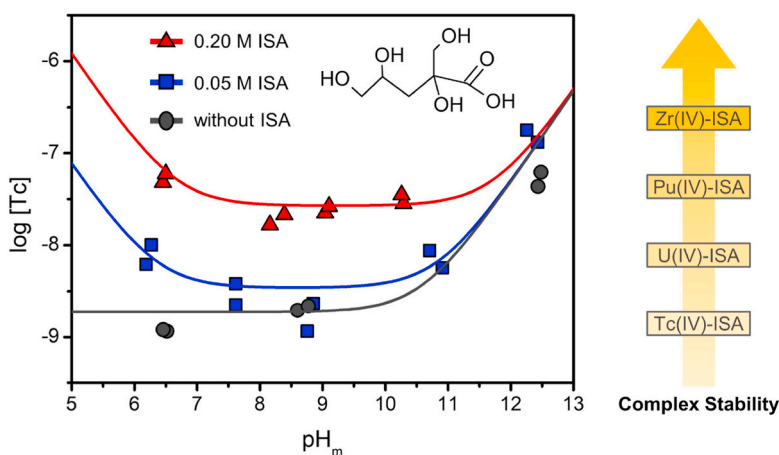[c] Pohang University of Science and Technology, Division of Environmental Science & Engineering, Pohang, 37673, Republic of Korea
[d] Pohang University of Science and Technology, Nuclear Environmental Technology Institute, Pohang, 37673, Republic of Korea

HIGHLIGHTS

- Isosaccharinic acid (ISA) is a cellulosic degradation product that increases the mobility of radionuclides in repositories.
- Complexation of ISA with Tc(IV) increased the solubility of Tc(IV) in neutral to weakly alkaline conditions.
- Thermodynamic model of Tc-ISA complexes, $TcO(OH)(ISA)_2^-$ and $TcO(OH)_2(ISA)_2^{2-}$ was derived.
- Tc(IV) forms weaker complexes with ISA than other M(IV) (M = Zr, Pu, U) due to its strong hydrolysis and predominance of TcO^{2+}.

GRAPHICAL ABSTRACT

ABSTRACT

Isosaccharinic acid (HISA, or ISA in its deprotonated form) is the main degradation product of cellulose under alkaline conditions. It can form strong complexes with radionuclides and other toxic metal ions, eventually enhancing their mobility in the context of nuclear waste repositories and other environmental systems. ^{99}Tc is a redox-sensitive, long-lived fission product produced in high yield in nuclear reactors. The solubility of ^{99}Tc(IV) was investigated in 0.5 M NaCl–NaISA–NaOH solutions with $6 \leq pH_m \leq 12.5$ and 10^{-6} M $\leq$ [ISA] ≤ 0.2 M. Complete chemical and thermodynamic models were derived on the basis of solubility data, (pe + pH_m) measurements, redox speciation, and solid phase characterization. These models include the previously unreported aqueous complexes $TcO(OH)(ISA)_2^-$ and $TcO(OH)_2(ISA)_2^{2-}$. In spite of the small size and high polarizability of the Tc^{4+} metal ion, the Tc(IV)-ISA complexes described in this work are significantly weaker than other ISA

* Corresponding author. Pohang University of Science and Technology, Division of Advanced Nuclear Engineering, Pohang, Republic of Korea.
** Corresponding author. Karlsruhe Institute of Technology, Institute for Nuclear Waste Disposal, Eggenstein-Leopoldshafen, 76344, Germany.
E-mail addresses: wooyongum@postech.ac.kr (W. Um), xavier.gaona@kit.edu (X. Gaona).

complexes formed with larger M^{4+} metal ions, *i.e.*, Zr, Pu and U. This unexpected behavior can be possibly explained by the strong hydrolysis of Tc(IV) and corresponding stabilization of the TcO^{2+} moiety, which does not occur for other M(IV) systems. Thermodynamic data derived in this work can be implemented in geochemical calculations of relevance in the context of nuclear waste disposal and other environmental applications.

1. Introduction

Technetium-99 (^{99}Tc) is a low-energy β emitter generated in nuclear reactors from the fission of ^{235}U and ^{239}Pu, as well as by neutron activation of molybdenum isotopes (Icenhower et al., 2008). It is also one of the radionuclides of concern in the management and disposal of radioactive waste owing to its long half-life ($t_{1/2} = 2.1 \times 10^5$ a) and redox-sensitive character (Desmet and Myttenaere, 1986). In aqueous systems and the absence of chelating ligands, Tc is predominantly found in the +VII and +IV oxidation states, with remarkably different chemical behavior. Tc(VII) prevails in weakly reducing to oxidizing conditions as pertechnetate ion (TcO_4^-), which is characterized by high solubility and mobility. Tc(IV) is expected to be the predominant oxidation state in the reducing conditions foreseen in underground repositories after closure. Tc(IV) is a hard Lewis acid, and accordingly characterized by a strong hydrolysis and the formation of sparingly soluble amorphous hydrous oxides, *i.e.*, TcO_2(am, hyd) (Baumann et al., 2018; Yalçıntaş et al., 2016).

A variety of organic materials are disposed of in repositories for low- and intermediate-level radioactive wastes (L/ILW), including decontamination agents (EDTA, NTA, citrate, etc.), cellulosic materials, ion exchange resins, plastic, rubber, among others (Glaus et al., 1999; Hummel et al., 2005; Maset et al., 2006). In the hyperalkaline conditions defined by cementitious systems used for repositories, cellulosic materials are chemically unstable and degrade, consequently producing soluble low-molecular-weight species (Bradbury and Van Loon, 1997). Isosaccharinic acid (HISA, $C_6H_{12}O_6$) comprises 70%–80% of the degradation products of cellulose in calcium-bearing alkaline solutions (Bradbury and Van Loon, 1997; Glaus and Van Loon, 2008; Pavasars et al., 2003). In alkaline to hyperalkaline conditions, ISA ($C_6H_{11}O_6^-$, as deprotonated form of HISA) has been shown to form strong complexes with metal ions, including actinides (*e.g.*, Th, U, Pu, Am) (Allard and Ekberg, 2006; Kim et al., 2022; Kobayashi et al., 2019; Rai et al., 2009; Tasi et al., 2018a, 2018b; Tits et al., 2005; Warwick et al., 2024), lanthanides (*e.g.*, Eu) (Vercammen et al., 2001) or transition metals (*e.g.*, Zr, Ni, Fe, etc.) (Evans et al., 2012; González-Siso et al., 2018; Kobayashi et al., 2017; Rai et al., 2012; Warwick et al., 2003). The chelating properties of ISA in alkaline to hyperalkaline systems are related to its large number of alcohol groups, which readily deprotonate in the presence of a strong Lewis acid, and thus are able to outcompete the hydrolysis of the metal ion. Metal-ISA complexation may enhance the solubility of a given radionuclide, and thus promote its mobilization from the repository into the biosphere.

Experimental studies reporting thermodynamic data for the complexation of selected organic ligands (EDTA, citrate, oxalate, ISA) with radionuclides were critically reviewed in volume 9 of the thermochemical database project of the Nuclear Energy Agency (NEA-TDB) in 2005 (Hummel et al., 2005). For Tc, the authors concluded that "No thermodynamic data on technetium isa compounds or complexes were identified in the literature." The recent study by Rai and Kitamura (2017) provided a thorough review of thermodynamic data available for the complexation of ISA with actinides, Fe and Ca, but did not report on the complexation with Tc. Indeed, literature focusing on the interaction of Tc with ISA is very scarce. The chemical reduction of pertechnetate and perrhenate in the presence of organic co-contaminants (EDTA, NTA, ISA) was investigated by Maset et al. (2006). The authors reported that pertechnetate was chemically reduced by Sn(II) within 3 d, leading to the formation of Tc(IV)-organic complexes, although the stoichiometry and stability of these complexes were not characterized. Technetium

(Z = 43) and zirconium (Z = 40) in the oxidation state +IV present evident similarities in their aqueous chemistry, mostly driven by the same (high) charge and relatively small ionic radii, i.e., $r_{Tc4+} = 0.645$ Å and $r_{Zr4+} = 0.72$ Å (both with coordination number, CN = 6) (Shannon, 1976). Both metal ions are characterized by a strong hydrolysis with the formation of anionic species in hyperalkaline conditions. The interaction of Zr(IV) with ISA was comprehensively investigated (Kobayashi et al., 2017). Based on a series of undersaturation solubility experiments, Kobayashi and co-workers reported the predominance of the complexes, $Zr(OH)_4(ISA)_2^{2-}$ and $Zr(OH)_4(ISA)(ISA_{-H})^{3-}$ in the near-neutral and alkaline pH-regions, respectively, in the presence of 10^{-3}–0.1 M ISA. The formation of analogous complexes might be expected for the Tc(IV)-ISA system.

In this context, this study aims at quantitatively evaluating the solubility, redox behavior and complexation of Tc in the presence of ISA. For this purpose, undersaturation solubility experiments were performed in the near-neutral to hyperalkaline, reducing conditions expected in underground repositories for radioactive waste disposal. Based on a combination of solubility data, redox speciation and solid phase characterization, chemical, thermodynamic and specific ion interaction theory (SIT) activity models were derived for the Tc^{4+}-Na^+-ISA^--OH^--Cl^--H_2O(l) system. These models can be implemented in geochemical calculations and used for the prediction of Tc behavior in cementitious systems containing cellulose.

2. Materials and methods

2.1. Chemicals and materials

Sodium chloride (NaCl, Merck, ≥99.5%), tin(II) chloride (SnCl₂, Sigma-Aldrich, 98%), sodium hydroxide (NaOH, Merck Titrisol), and hydrochloric acid (HCl, Merck Titrisol) were used to prepare sample solutions. Calcium alpha-ᴅ-isosaccharinate (Ca(ISA)₂, $C_{12}H_{22}CaO_{12}$, Alfa Aesar, 98%), Chelex® 100 Resin (50–100 mesh, sodium form, Bio-Rad) and diethyl ether ($C_4H_{10}O$, Sigma-Aldrich, ≥99%) were obtained to synthesize sodium isosaccharinate (NaISA, $C_6H_{11}NaO_6$). The solid phase used in this study, TcO_2(am, hyd), was synthesized by electrochemical reduction of a Tc(VII) stock solution in 1.0 M HCl, followed by precipitation in a 4 M NaOH solution containing 10 mM Sn(II), as described in Baumann et al. (2018). Tetraphenylphosphonium chloride (TPPC, $C_{24}H_{20}ClP$, Sigma-Aldrich, 98%) was dissolved in chloroform (CHCl₃, Sigma-Aldrich, ≥99%) and used for Tc(IV) quantification via solvent extraction. Liquid scintillation counting (LSC) was performed using an LSC cocktail (Ultima Gold™ XR, PerkinElmer).

All experiments were performed in controlled laboratories at the Institute for Nuclear Waste Disposal at the Karlsruhe Institute of Technology (KIT-INE). Technetium solubility experiments were conducted in an argon glovebox with <3 ppm O₂ at T = (22 ± 2) °C. All sample solutions were prepared with ultra pure water from Millipore Milli-Q Advantage A10 (18.2 MΩ·cm at 25 °C), which was purged with Ar for 3 h before use.

2.2. Synthesis of NaISA

NaISA was prepared according to the synthesis method described in Chew and Van Loon et al. (Chew, 2013; Van Loon and Glaus, 1998). Briefly, the calcium ions of commercial Ca(ISA)₂ were exchanged with sodium by reacting with ion exchange resin in Milli-Q water, and the filtrate was evaporated to obtain the NaISA solid phase. The resulting
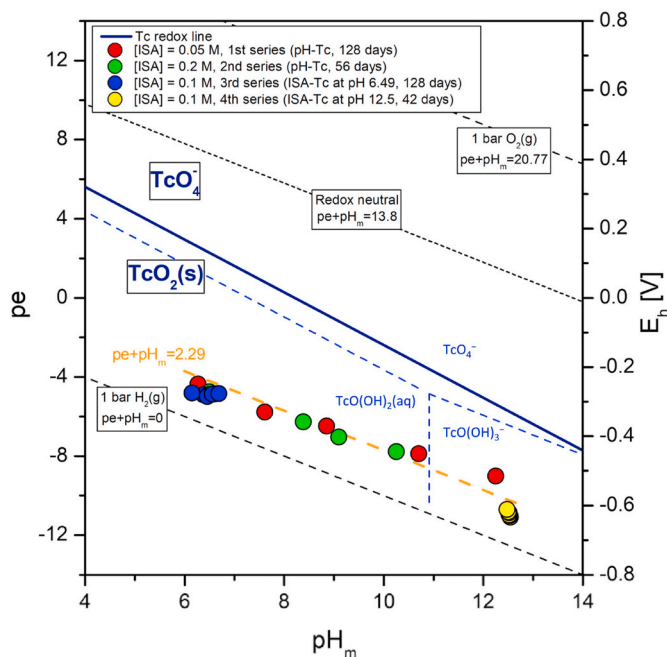
Fig. 1. All investigated Tc-ISA data with the measured values of pe + pH$_m$. Experimental data plotted in the Pourbaix diagram of Tc calculated at [Tc] = 10^{-5} M and I = 0.5 M using the thermodynamic data selection in NEA-TDB (Grenthe et al., 2020). Dark blue solid line corresponds to the calculated redox border line of Tc, with Tc(IV):Tc(VII) = 1:1. Blue dashed lines indicate the borderline of aqueous Tc species. Black dashed lines delimit the stability field of water, with (pe + pH) = 20.77 and 0. The redox-neutral line at (pe + pH = 13.8) is shown for comparison. (For interpretation of the references to colour in this figure legend, the reader is referred to the Web version of this article.)

crystals were characterized by X-ray diffraction, nuclear magnetic resonance, and Fourier Transform Infrared spectroscopy, which confirmed the successful synthesis of NaISA. A detailed description of the procedure for the synthesis and characterization of NaISA is provided in the Supplementary material (S-1).

2.3. pH$_m$ and E$_h$ measurements

The values of pH were determined using a ROSS combination pH electrode (Thermo Scientific, Orion™), calibrated with standard buffer solutions (pH = 4 to 10, Merck). In aqueous systems with ionic strength $I \geq 0.1$ M, the experimentally measured pH (pH$_{exp}$) is an operational apparent value related to the molal proton concentration by pH$_m$ = pH$_{exp}$ + A$_m$, with pH$_m$ = –log [H$^+$] and [H$^+$] in mol•kg^{-1}. A$_m$ are empirical values entailing both the activity coefficient of H$^+$ and the liquid junction potential of the electrode for a given background electrolyte concentration. A$_m$ values in NaCl solutions used in this work were previously reported by Altmaier et al. (2003).

The redox potential was measured using a Pt combination electrode with an Ag/AgCl reference system (Metrohm). The performance of the redox electrode was tested before use with a standard redox buffer solution (+220 mV vs. Ag/AgCl, Schott), which provided readings within ±10 mV of the certified value. All samples were measured for 10–20 min while gently stirring. The measured redox potential was converted to the redox potential (E_h) versus the standard hydrogen electrode (SHE) by correcting for the potential of the Ag/AgCl reference electrode (+207 mV for 3 M KCl at 25 °C). The apparent electron activity (pe = – log a_{e^-}) was calculated as pe = 16.9 E_h [V], based on the equation $E_h = \frac{RT \ln(10)}{F}$ pe.

2.4. Tc-ISA solubility experiments

Undersaturation solubility experiments were conducted with synthetic TcO$_2$(am, hyd). Ionic strength was fixed in all systems at I = 0.5 M, considering the contributions of all major components in the system (NaCl–NaOH-NaISA-HCl). For all samples, 2 mM SnCl$_2$ was added to ensure reducing conditions and prevent oxidation of Tc(IV) to Tc(VII). The pH$_m$ was adjusted using NaOH and HCl solutions with the same ionic strength and monitored to confirm stable readings prior to the addition of Tc. Then, 2–3 mg of solid TcO$_2$(am, hyd) was washed three times with 1 mL of the background solution, and added to 10 mL of the background solution in polypropylene vessels. Four independent series of solubility experiments were prepared in the presence of ISA: (i) [ISA] = 0.05 M, 6 ≤ pH$_m$ ≤ 12.5; (ii) [ISA] = 0.2 M, 6 ≤ pH$_m$ ≤ 10.5; (iii) pH$_m$ = 6.5, 10^{-6} M ≤ [ISA] ≤ 0.2 M; and (iv) pH$_m$ = 12.5, 10^{-6} M ≤ [ISA] ≤ 0.1 M. Three additional samples were prepared in the absence of ISA and 6.5 ≤ pH$_m$ ≤ 12.5. The pH$_m$, E_h, and Tc concentration were monitored at regular time intervals for up to 128 d.

Tc concentration was measured by means of liquid scintillation counting (LSC). A defined amount of supernatant (500 µL) was filtered and centrifuged through a 10 kD centrifugal filter (2–3 nm cut-off, Nanosep®, and Mikrosep® Pall Life Sciences) for 5 min at 4020 g to remove colloids or residual solid particles. After mixing 400 µL of filtrate with 600 µL of HCl (1.0 M), 600 µL of the mixed solution was added to 10 mL of LSC cocktail in a polypropylene vial (20 mL, Zinsser Analytic) and agitated by hand. The resulting sample was analyzed for 30 min using an LKB Wallac 1220 Quantulus LSC (PerkinElmer). A detection limit of [Tc] ≈ 10^{-9} M was calculated as three times the standard deviation of five blank samples.

2.5. Redox speciation and solid phase characterization

A solvent extraction method with tetraphenylphosphonium chloride (TPPC) dissolved in chloroform was used to determine the concentration of Tc(IV) in the aqueous phase. TPPC is an extraction ligand forming very stable, anhydrous ion-pair complexes with TcO$_4^-$. Tc(IV) concentration in the aqueous phase can be accordingly quantified after extracting Tc(VII) into the organic phase (Hess et al., 2004; Kopunec et al., 1998; Xia et al., 2006). After phase separation (10 kD ultrafiltration) of selected samples, 500 µL of the filtrate was contacted with 500 µL of chloroform containing 0.05 mM TTPC and shaken vigorously for 1 min. From the separated aqueous phase, 400 µL was pipetted and mixed with 600 µL of 1.0 M HCl. For Tc(IV) concentration measurement, 600 µL of the mixed solution was added to 10 mL of LSC cocktail and measured for 30 min by an LKB Wallac 1220 Quantulus LSC.

After attaining equilibrium conditions, confirmed by stable pH$_m$, E_h and [Tc] measurements, selected solid phases were characterized by X-ray diffraction (XRD). An aliquot of each Tc solid phase (~1 mg) was washed with Milli-Q water three times to remove the remaining salt-containing background solution of the samples and prevent interference with the characterization. The washed solid phase was suspended in a small amount of Milli-Q water and dried on a sample holder inside a glovebox. After the evaporation of the solution, the sample was transferred outside of the glovebox and measured using a Bruker AXS D8 Advance X-ray powder diffractometer (Cu-Kα radiation, LynxEye XE-T detector). Diffraction patterns were collected for 2° < 2θ < 80°, with incremental steps of 0.02° and a measurement time of 0.5 s/step.

2.6. Thermodynamic data and ionic strength corrections

Thermodynamic data in the reference state describing the Tc^{4+}-Na$^+$-ISA$^-$-OH$^-$-Cl$^-$-H$_2$O(l) system were determined on the basis of solubility data obtained in this work at I = 0.5 M. The SIT was used to account for ionic strength corrections (Ciavatta, 1980; Hummel, 2009). In SIT, the activity coefficient of an i ion is calculated based on the Debye−Hückel equation and the specific short-range interaction between charged ions,
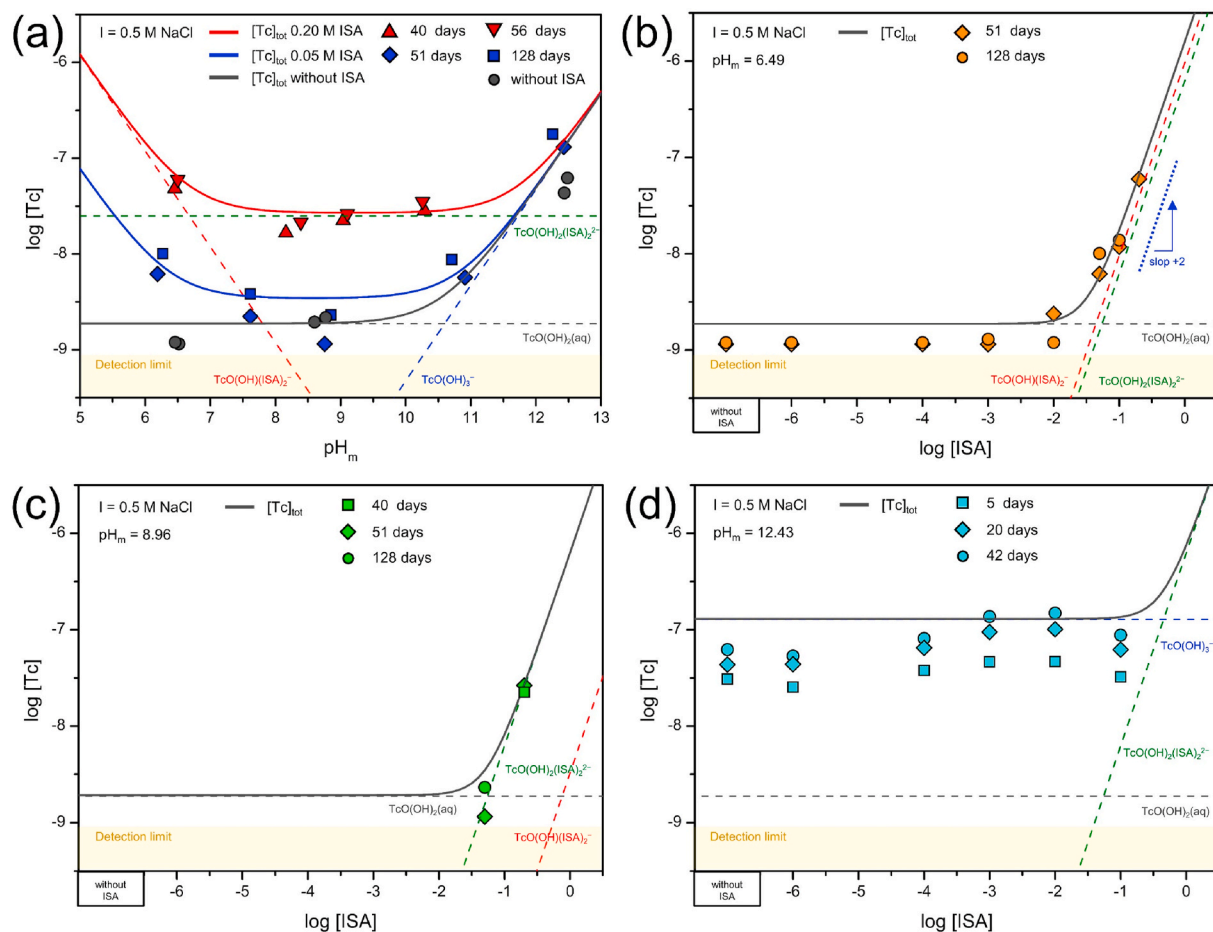
Fig. 2. Experimental Tc solubility data (a) at varying pH_m with [ISA] = 0.05 M (blue symbols), [ISA] = 0.2 M (red symbols), and in the absence of ISA (black symbols); and with varying ISA concentration at (b) pH_m = 6.49, (c) pH_m = 8.96, and (d) pH_m = 12.43. Solid lines correspond to the calculated TcO_2(am, hyd, aged) solubility curve at I = 0.5 M NaCl using the thermodynamic selection in NEA-TDB (ISA-free systems) and the thermodynamic model derived in this study for the Tc (IV)-ISA system. Dashed lines represent the calculated concentrations of Tc(IV) aqueous species at I = 0.5 M NaCl. (For interpretation of the references to colour in this figure legend, the reader is referred to the Web version of this article.)

Table 1

Solubility constants determined in this work for the Tc(IV)-ISA systems, and complexation constants recalculated using thermodynamic data selected in the NEA-TDB (Grenthe et al., 2020).

Chemical reaction	log $*K°$
TcO_2(am, hyd, aged) + 2 ISA^- + H^+ ⇌ $TcO(OH)(ISA)_2^-$	(0.8 ± 0.1)
TcO_2(am, hyd, aged) + 2 ISA^- + $H_2O(l)$ ⇌ $TcO(OH)_2(ISA)_2^{2-}$	–(6.5 ± 0.1)
$TcO(OH)_2$(aq) + 2 ISA^- + H^+ ⇌ $TcO(OH)(ISA)_2^-$ + $H_2O(l)$	(9.5 ± 0.5)
$TcO(OH)_2$(aq) + 2 ISA^- ⇌ $TcO(OH)_2(ISA)_2^{2-}$	(2.2 ± 0.5)

$log\, \gamma_i = -\, z_i^2 \frac{0.509\sqrt{I}}{1+1.5\sqrt{I}} + \sum_j \varepsilon(i,j)\, m_j$, where the concentration of the oppositely charged ion m_j is $\approx I$ in the case of 1:1 electrolytes. The validity range of SIT is usually considered within $I \leq 3.5$ M (Anderegg and Kholeif, 1994), although accurate ionic strength corrections have been also proven for 1:1 and 1:2 electrolytes with $I \leq 13.5$ M (Yalçıntaş et al., 2016; Fellhauer et al., 2010). Thermodynamic data for Tc(IV) solubility and hydrolysis, as well as selected ion interaction coefficients used in this study were obtained from the recent NEA-TDB Update book (Grenthe et al., 2020) and previously estimated coefficients (Rai et al., 2012). The ion interaction coefficients for the Tc(IV)-ISA complexes described in this work were estimated based on charge considerations, as previously described by Hummel (2009).

3. Results and discussion

3.1. (pe + pH_m) measurements and Tc redox speciation

Experimentally measured pH_m and pe values for all investigated systems are shown in the Pourbaix diagram of Tc in Fig. 1, calculated with the thermodynamic data summarized in Table S-4 in the Supplementary material. The use of Sn(II) as a reductant ensured strongly reducing conditions, i.e. (pe + pH_m) = (2.3 ± 0.2), close to the border of water reduction. These values are close to those reported in the literature for ISA-free systems, i.e., (pe + pH_m) ≈ 2 (Yalçıntaş et al., 2015). In all cases, the measured (pe + pH_m) values are well below the thermodynamically calculated redox border-line between Tc(IV) and Tc(VII), thus supporting the predominance of the +IV oxidation state in the Tc-ISA systems investigated.

The redox speciation of Tc in the aqueous phase was determined by means of solvent extraction with TPPC. The measured Tc(IV) and total Tc concentrations are summarized in Table S-5. The average Tc(IV) percentage of total Tc concentration was (100 ± 10) %, thus confirming the prevalence of the +IV oxidation state in the aqueous phase, as foreseen based on (pe + pH_m) measurements and thermodynamic calculations.

3.2. Solubility experiments and solid phase characterization

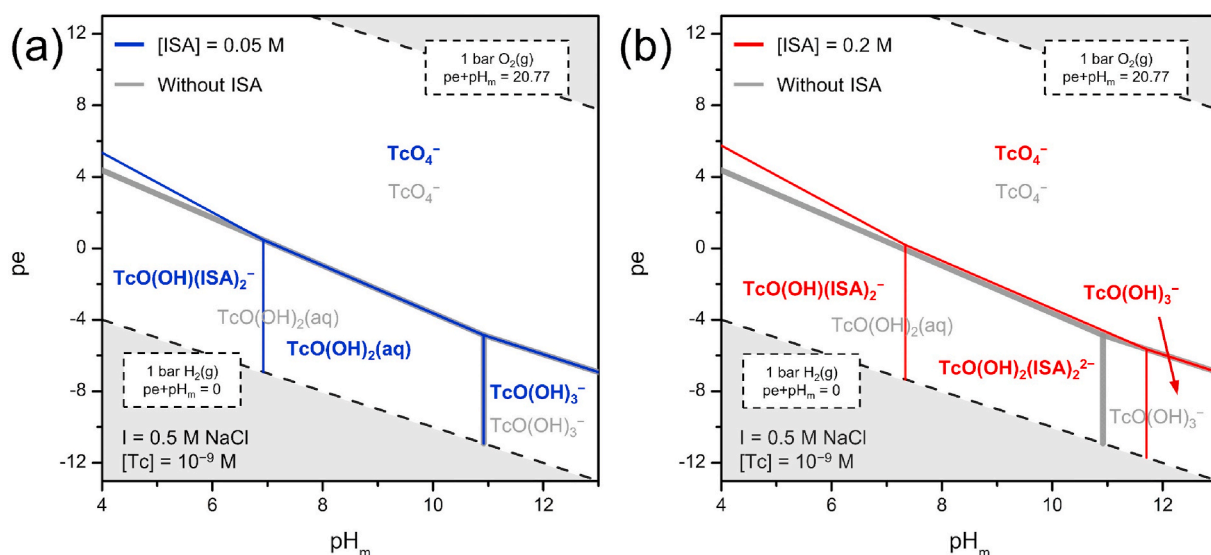Experimental solubility data collected at constant [ISA] (0.05 and

Fig. 3. Pourbaix diagrams of Tc calculated at $[Tc]_{tot} = 10^{-9}$ M, $5 \leq pH_m \leq 13$ and $I = 0.5$ M NaCl in the presence of (a) [ISA] = 0.05 M and (b) [ISA] = 0.2 M, using thermodynamic data selected in the NEA-TDB and derived in this work.

0.2 M) and varying pH_m ($6 \leq pH_m \leq 12.5$) are shown in Fig. 2a, whereas Fig. 2b–d displays solubility data determined at constant pH_m (~6.5, ~9 and ~12.4) and varying ISA concentration (10^{-6} M $\leq$ [ISA] ≤ 0.2 M). Tc concentrations monitored as a function of time confirmed that equilibrium conditions were attained after approximately 40 d (see Figure S-5).

Tc concentrations in the absence of ISA are in moderate agreement with the solubility calculated for TcO_2(am, hyd, aged) using the current NEA-TDB selection (Fig. 2a). Experiments conducted in the presence of [ISA] = 0.2 M show a clear enhancement of Tc concentrations (compared to ISA-free systems) at $pH_m \leq 11$, which is attributed to the formation of Tc(IV)-ISA complex/es. The pH_m-independent solubility observed within $8 \leq pH_m \leq 10$ indicates that the chemical reaction controlling the solubility in this pH_m-region involves no exchange of H$^+$. The increase in the solubility is more accentuated in near-neutral pH_m conditions, where solubility experiments in the presence of [ISA] = 0.05 M show also a significant increase in [Tc] with respect to ISA-free systems. This observation hints towards the predominance of a different Tc(IV)-ISA species in the aqueous phase, and to a chemical reaction involving the uptake of H$^+$. In contrast to these observations, all solubility experiments conducted at $pH_m \approx 12.4$ show a negligible impact of ISA up to a ligand concentration of 0.2 M (see Fig. 2a and d). These results confirm that complexation with ISA cannot outcompete Tc(IV) hydrolysis under hyperalkaline conditions, where the anionic species $TcO(OH)_3^-$ prevails. Similar observations were recently reported by DiBlasi et al. (2023) for the systems Tc(IV)-EDTA, Tc(IV)-NTA and Tc(IV)-citrate.
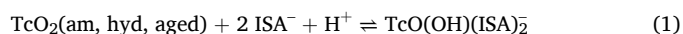
Fig. 2b and c shows the evolution of the Tc solubility with increasing ISA concentrations at $pH_m \approx 6.5$ and ≈ 9. In both cases, the increase in solubility follows a well-defined slope of ~2, thus hinting towards the formation of Tc(IV)-ISA complexes with a stoichiometry 1:2. Consistently with the results shown in Fig. 2a, the threshold ISA concentration promoting an increase in the Tc solubility is lower at $pH_m \approx 6.5$ than at $pH_m \approx 9$.

Solid phases of selected solubility samples in the presence of ISA were characterized by means of XRD (see Figure S-6). The diffractograms of the solid phases equilibrated at pH = 6.27 and 10.7 show no remarkable patterns, thus reflecting the amorphous character of the Tc solids. The minor diffraction peaks at $2\theta \approx 18.3°$ and $37.1°$ for the solid phase at pH = 6.27 agree well with reference patterns for SnO(cr), owing to the low solubility of Sn(II) under neutral conditions (Duckworth et al., 2021). The combination of (pe + pH_m) measurements, thermodynamic calculations, solvent extraction data, XRD analyses as well as

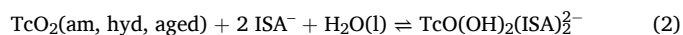experimental solubility data in ISA-free systems support that TcO_2(am, hyd, aged) is the solid phase controlling the solubility in all investigated systems.

3.3. Thermodynamic description of the Tc(IV)-ISA complexes

On the basis of solubility data determined in this work, slope analyses (as log [Tc] vs. pH_m and log [Tc] vs. log [ISA]), and considering a solubility control by TcO_2(am, hyd, aged), a chemical model including the aqueous species of $TcO(OH)(ISA)_2^-$ and $TcO(OH)_2(ISA)_2^{2-}$ was defined according with the chemical reactions (1) and (2):

$$TcO_2(am,\ hyd,\ aged) + 2\ ISA^- + H^+ \rightleftharpoons TcO(OH)(ISA)_2^- \qquad (1)$$

(slope -1: log [Tc(IV)] vs. pH_m // slope $+2$: log [Tc(IV)] vs. log $[ISA^-]_{free}$)

$$TcO_2(am,\ hyd,\ aged) + 2\ ISA^- + H_2O(l) \rightleftharpoons TcO(OH)_2(ISA)_2^{2-} \qquad (2)$$

(slope 0: log [Tc(IV)] vs. pH_m // slope $+2$: log [Tc(IV)] vs. log $[ISA^-]_{free}$)

Note that within the boundary conditions in this study, $[ISA^-]_{free} \approx [ISA^-]_{total}$ due to the negligible contribution of other ISA species, i.e., HISA(aq) or ISA-lactone. Tc(IV)-ISA complexes in reactions (1) and (2) can be equally defined claiming the deprotonation of one alcohol group of ISA instead of the hydrolysis of the Tc(IV) metal ion, i.e., $TcO(ISA_{-H})(ISA)^-$ instead of $TcO(OH)(ISA)_2^-$, or $TcO(ISA_{-H})_2^{2-}$ instead of $TcO(OH)_2(ISA)_2^{2-}$. In both cases, the stoichiometry of the chemical reaction remains the same (with the exception of the number of water molecules), thus having no implications for the thermodynamic functions accordingly derived. Based on the equilibrium reactions (1) and (2) above, the corresponding conditional solubility constants at $I = 0.5$ M can be calculated as:

$$\log {}^*K'_{s,(1,1,2)} = \log [TcO(OH)(ISA)_2^-] + pH_m - 2\log [ISA^-] \qquad (3)$$

$$\log {}^*K'_{s,(1,2,2)} = \log [TcO(OH)_2(ISA)_2^{2-}] - 2\log [ISA^-] \qquad (4)$$

and the corresponding solubility constants at the reference state, where $\gamma(M)$ denotes the activity coefficient of the ion M and a_w indicates the activity of water:

$$\log {}^*K°_{s,(1,1,2)} = \log {}^*K'_{s,(1,1,2)} + \log \gamma(TcO(OH)(ISA)_2^-) - \log \gamma(H^+) - 2\log \gamma(ISA^-) \qquad (5)$$

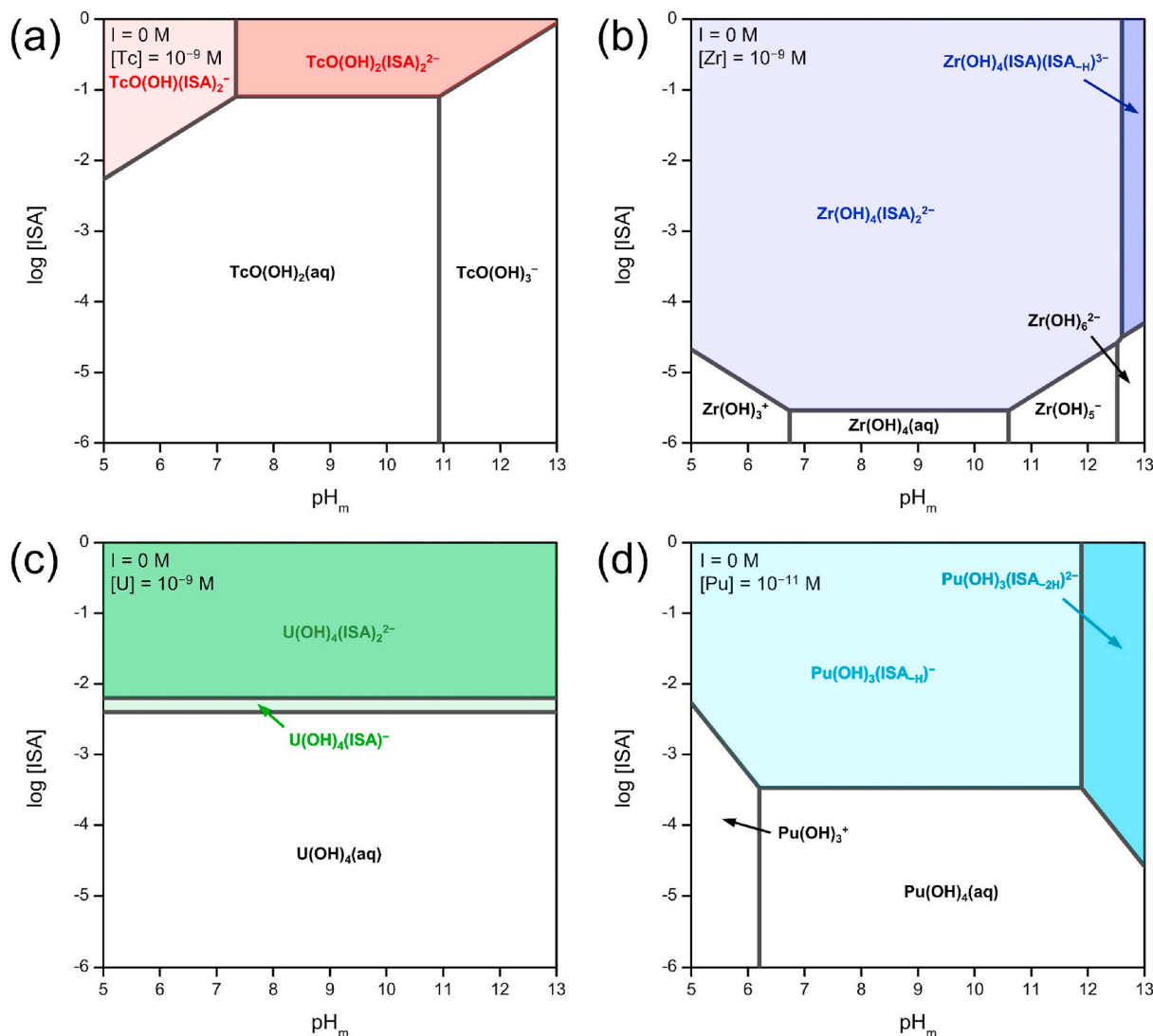**Fig. 4.** Predominance diagrams of M(IV) systems in the presence of ISA ($-6 \leq$ log [ISA] ≤ 0) and $5 \leq$ pH$_m \leq 13$ at $I = 0$ M, calculated with thermodynamic data available for (a) Tc(IV) (this work), (b) Zr(IV) (Kobayashi et al., 2017), (c) U(IV) (Kobayashi et al., 2019), and (d) Pu(IV) (Tasi et al., 2018a).

$$\log *K^\circ_{s,(1,2,2)} = \log *K'_{s,(1,2,2)} + \log \gamma(\text{TcO(OH)}_2(\text{ISA})_2^{2-}) - 2 \log \gamma(\text{ISA}^-)$$
$$- \log a_w \tag{6}$$

The conditional solubility constants $*K'_{s,(1,1,2)}$ and $*K'_{s,(1,2,2)}$ were obtained by minimizing the difference between experimental and calculated solubility, according to the following function:

$$f\left(*K'_{s,(1,1,2)}, *K'_{s,(1,2,2)}\right) = \sqrt{\sum_{i=1}^{n}\left[\left(\log [\text{Tc}]_{tot}^{exp,i} \text{-log } [\text{Tc}]_{tot}^{cal,i}\right)^2\right]} \tag{7}$$

Conditional solubility constants determined at $I = 0.5$ M were extrapolated to $I \rightarrow 0$ according to equations (5) and (6) and using SIT for the calculation of the activity coefficients of the ionic species. The SIT ion interaction coefficients for the Tc(IV)-ISA aqueous complexes are not available, and were estimated as $\varepsilon(\text{Na}^+, \text{TcO(OH)(ISA)}_2^-) = -(0.05 \pm 0.10)$ kg·mol^{-1} and $\varepsilon(\text{Na}^+, \text{TcO(OH)}_2(\text{ISA})_2^{2-}) = -(0.10 \pm 0.10)$ kg·mol^{-1} based on charge analogies (Hummel, 2009). The resulting solubility constants in the reference state, as well as the re-calculated complexation constants are summarized in Table 1.

The solubility of TcO$_2$(am, hyd, aged) in the presence of ISA calculated using the thermodynamic constants derived in this study satisfactorily explains all experimental observations (see Fig. 2). The species TcO(OH)(ISA)$_2^-$ is responsible for the increase in Tc concentration at pH$_m < 8$ and [ISA] $\geq 10^{-2}$ M, whereas the complex TcO(OH)$_2$(ISA)$_2^{2-}$

prevails above this pH$_m$ and up to pH$_m$ values of ~11 (depending upon ISA concentration).

Pourbaix diagrams for the Tc-ISA system calculated using thermodynamic data derived in this work are shown in Fig. 3a and b. As discussed above, Tc(IV)-ISA complexes become exclusively predominant at high ISA concentrations, and only at pH$_m < 11$. Above this pH$_m$, the formation of the anionic hydrolysis species TcO(OH)$_3^-$ outcompetes Tc (IV)-ISA complexes, at least for [ISA] ≤ 0.2 M. This behavior significantly differs from previous studies with other M(IV)-ISA systems. Fig. 4 shows the predominance diagrams for M(IV)-ISA complexes, with M = Tc (this work), Zr (Kobayashi et al., 2017), U (Kobayashi et al., 2019) and Pu (Tasi et al., 2018a). Although acknowledging the differences between the corresponding chemical models, thermodynamic calculations in Fig. 4 evidence that the stability of the M(IV)-ISA complexes follows the sequence: Zr(IV)-ISA $\gg$ Pu(IV)-ISA $>$ U(IV)-ISA $>$ Tc (IV)-ISA. Indeed, the stability of the Tc(IV)-ISA complexes is even weaker than those reported for Ni(II) (González-Siso et al., 2018), a Lewis acid significantly weaker than Tc(IV) (see Figure S-7b).

When accounting for complexes of M(IV) with organic ligands where the electrostatic contribution prevails, a linear dependence of log $*\beta^\circ$ values with the polarizability of the metal ion, expressed in terms of its charge density (z^2/r_i) or as the reciprocal of its ionic radii ($1/r_i$) is

foreseeable (Gaona et al., 2008). Considering the ionic radii of the M(IV) metal ions under discussion, *i.e.*, $r_{Tc4+} = 0.645$ Å (CN = 6) $< r_{Zr4+} = 0.72$ Å (CN = 6) $\ll r_{Pu4+} = 1.01$ Å (CN = 8) $\approx r_{U4+} = 1.04$ Å (CN = 8) (Shannon, 1976; Neck and Kim, 2001), this trend is confirmed for the Zr (IV)-ISA, Pu(IV)-ISA and U(IV)-ISA systems. On the other hand, the Tc (IV)-ISA system completely falls out of the trend, as the highest stability of all evaluated M(IV)-ISA systems would be expected based on the smallest ionic radii of the Tc^{4+} cation. We note that as a consequence of its very strong hydrolysis, the predominance of the moiety TcO^{2+} is described already in very acidic conditions and is proposed to remain stable up to hyperalkaline conditions, *e.g.*, in the form of $TcO(OH)_2(aq)$ or $TcO(OH)_3^-$ (Grenthe et al., 2020). In contrast to this, all other M(IV) exist as clean M^{4+} ions. We speculate that the stability of the TcO^{2+} moiety hinder the formation of more stable complexes in the Tc(IV)-ISA system, in spite of the large polarizability of the Tc^{4+} cation. Dedicated density functional theory calculations may help in the future to validate or reject this hypothesis.

4. Conclusions

The complexation of Tc(IV) with ISA under reducing conditions was systematically investigated for the first time. ISA is the main degradation product of cellulose in the cementitious environments expected in repositories for low and intermediate level radioactive waste.

Batch solubility experiments were conducted in four independent series under the variation of pH_m and ISA concentrations. Experimentally measured (pe + pH) values, in combination with thermodynamic calculations and solvent extraction methods confirmed the predominance of Tc in the oxidation state + IV in the investigated reducing systems. Solubility experiments revealed a moderate to weak complexation of ISA with Tc(IV) in near-neutral to weakly alkaline pH_m conditions. Above $pH_m \approx 11$, the predominance of the anionic hydrolysis species $TcO(OH)_3^-$ outcompetes the formation of Tc(IV)-ISA complexes. Chemical and thermodynamic models derived in this work include the previously unreported Tc complexes, $TcO(OH)(ISA)_2^-$ and $TcO(OH)_2(ISA)_2^{2-}$. The comparison with previous studies dealing with M (IV)-ISA systems (with M = Zr, U and Pu) evidences that Tc falls out of the trend defined by the size and polarizability of the metal ion. This observation is explained by the very strong hydrolysis of Tc(IV) and the stabilization of the moiety TcO^{2+}, which expectedly forms weaker complexes with ISA than the M^{4+} cations prevailing for all other M(IV) systems considered.

Thermodynamic data derived in this study can be implemented in thermodynamic databases and geochemical calculations of relevance in the context of nuclear waste disposal, whilst providing a fundamental understanding on the systematics behind the complexation of the strongly hydrolyzing metal ions M(IV) with ISA.

CRediT authorship contribution statement

Kyungwon Kim: Writing – original draft, Investigation. **Sarah B. Duckworth:** Methodology, Data curation. **Marcus Altmaier:** Writing – review & editing, Supervision. **Wooyong Um:** Writing – review & editing, Project administration, Funding acquisition, Conceptualization. **Xavier Gaona:** Writing – review & editing, Supervision, Project administration, Funding acquisition, Conceptualization.

Declaration of competing interest

The authors declare that they have no known competing financial interests or personal relationships that could have appeared to influence the work reported in this paper.

Data availability

No data was used for the research described in the article.

Appendix B. Supplementary data

Supplementary data to this article can be found online at https://doi.org/10.1016/j.chemosphere.2024.143140.

References

Allard, S., Ekberg, C., 2006. Complexing properties of α-isosaccharinate: thorium. Radiochim. Acta 94 (9–11), 537–540. https://doi.org/10.1524/ract.2006.94.9-11.537.

Altmaier, M., Metz, V., Neck, V., Müller, R., Fanghänel, T., 2003. Solid-liquid equilibria of Mg(OH)₂(cr) and Mg₂(OH)₃Cl·4H₂O(cr) in the system Mg-Na-H-OH-Cl-H₂O at 25°C. Geochem. Cosmochim. Acta 67 (19), 3595–3601. https://doi.org/10.1016/S0016-7037(03)00165-0.

Anderegg, G., Kholeif, S., 1994. The extrapolation of experimental equilibrium constant data to zero ionic strength: critical review and new approach. Talanta 41 (9), 1507–1522. https://doi.org/10.1016/0039-9140(94)E0061-U.

Baumann, A., Yalçıntaş, E., Gaona, X., Polly, R., Dardenne, K., Pruessmann, T., Rothe, J., Altmaier, M., Geckeis, H., 2018. Thermodynamic description of Tc (IV) solubility and carbonate complexation in alkaline NaHCO₃–Na₂CO₃–NaCl systems. Dalton Trans. 47 (12), 4377–4392. https://doi.org/10.1039/C8DT00250A.

Bradbury, M.H., Van Loon, L.R., 1997. Cementitious Near-Field Sorption Data Bases for Performance Assessment of a L/ILW Repository in a Palfris Marl Host Rock. Paul Scherrer Institut. https://www.osti.gov/etdeweb/biblio/587843.

Chew, M., 2013. Investigation of Uranium Redox Chemistry and Complexation across the pH Range by Cyclic Voltammetry. Loughborough University, Thesis. https://hdl.handle.net/2134/13475.

Ciavatta, L., 1980. The specific interaction theory in evaluating ionic equilibria. Ann. Chim. (Rome) 70, 551.

Desmet, G., Myttenaere, C., 1986. Technetium in the Environment, vol. 10102. Springer Science & Business Media.

DiBlasi, N.A., Dardenne, K., Prüssmann, T., Duckworth, S., Altmaier, M., Gaona, X., 2023. Technetium complexation with multidentate carboxylate-containing ligands: trends in redox and solubility phenomena. Environ. Sci. Technol. 57 (9), 3661–3670. https://doi.org/10.1021/acs.est.2c09360.

Duckworth, S., Gaona, X., Castaño, D., Park, S., Altmaier, M., Geckeis, H., 2021. Redox chemistry, solubility and hydrolysis of Re in reducing aquatic systems. Thermodynamic description and comparison with Tc. Appl. Geochem. 132, 105037 https://doi.org/10.1016/j.apgeochem.2021.105037.

Evans, N., Gascón, S.A., Vines, S., Felipe-Sotelo, M., 2012. Effect of competition from other metals on nickel complexation by α-isosaccharinic, gluconic and picolinic acids. Mineral. Mag. 76 (8), 3425–3434. https://doi.org/10.1180/minmag.2012.076.8.55.

Fellhauer, D., Neck, V., Altmaier, M., Lützenkirchen, J., Fanghänel, T., 2010. Solubility of tetravalent actinides in alkaline CaCl₂ solutions and formation of Ca₄[An(OH)₈]⁴⁺ complexes: a study of Np(IV) and Pu(IV) under reducing conditions and the systematic trend in the An(IV) series. Radiochim. Acta 98 (9–11), 541–548. https://doi.org/10.1524/ract.2010.1751.

Gaona, X., Montoya, V., Colàs, E., Grivé, M., Duro, L., 2008. Review of the complexation of tetravalent actinides by ISA and gluconate under alkaline to hyperalkaline conditions. J. Contam. Hydrol. 102 (3–4), 217–227. https://doi.org/10.1016/j.jconhyd.2008.09.017.

Glaus, M.A., Van Loon, L.R., 2008. Degradation of cellulose under alkaline conditions: new insights from a 12 years degradation study. Environ. Sci. Technol. 42 (8), 2906–2911. https://doi.org/10.1021/es7025517.

Glaus, M., Van Loon, L., Achatz, S., Chodura, A., Fischer, K., 1999. Degradation of cellulosic materials under the alkaline conditions of a cementitious repository for low and intermediate level radioactive waste: Part I: identification of degradation products. Anal. Chim. Acta 398 (1), 111–122. https://doi.org/10.1016/S0003-2670(99)00371-2.

González-Siso, M.R., Gaona, X., Duro, L., Altmaier, M., Bruno, J., 2018. Thermodynamic model of Ni(II) solubility, hydrolysis and complex formation with ISA. Radiochim. Acta 106 (1), 31–45. https://doi.org/10.1515/ract-2017-2762.

Grenthe, I., Gaona, X., Plyasunov, A.V., Rao, L., Runde, W.H., Grambow, B., Konings, R.J. M., Smith, A.L., Moore, E.E., Ragoussi, M., Martinez, J.S., Costa, D., 2020. Second Update on the Chemical Thermodynamics of Uranium, Neptunium, Plutonium, Americium and Technetium. OECD/NEA Publishing.

Hess, N.J., Xia, Y., Rai, D., Conradson, S.D., 2004. Thermodynamic model for the solubility of TcO₂·xH₂O(am) in the aqueous Tc(IV)–Na⁺–Cl⁻–H⁺–OH⁻–H₂O system. J. Solut. Chem. 33, 199–226. https://doi.org/10.1023/B:JOSL.0000030285.11512.1f.

Hummel, W., 2009. Ionic Strength Corrections and Estimation of SIT Ion Interaction Coefficients. Paul Scherrer Institut, Villigen, Switzerland. PSI report TM-44-09-01.

Hummel, W., Anderegg, G., Rao, L., Puigdomènech, I., Yochiyama, O., Mompean, F.J., Illemassène, M., Perrone, J., 2005. Chemical thermodynamics of compounds and complexes of U, Np, Pu, Am, Tc, Se. In: Ni and Zr with Selected Organic Ligands, vol. 9. Elsevier, Amsterdam.

Icenhower, J.P., Qafoku, N., Martin, W.J., Zachara, J.M., 2008. The Geochemistry of Technetium: a Summary of the Behavior of an Artificial Element in the Natural Environment. Pacific Northwest National Lab.(PNNL), Richland, WA (United States).

Kim, H.-K., Cho, H., Jeong, K., Yoon, U.H., Cho, H.-R., 2022. Thermodynamic study of Am(III)–Isosaccharinate complexation at various temperatures implicating a stepwise reduction in binding denticity. Inorg. Chem. 61 (48), 19369–19378. https://doi.org/10.1021/acs.inorgchem.2c03180.

Kobayashi, T., Teshima, T., Sasaki, T., Kitamura, A., 2017. Thermodynamic model for Zr solubility in the presence of gluconic acid and isosaccharinic acid. J. Nucl. Sci. Technol. 54 (2), 233–241. https://doi.org/10.1080/00223131.2016.1255573.

Kobayashi, T., Sasaki, T., Kitamura, A., 2019. Thermodynamic interpretation of uranium (IV/VI) solubility in the presence of α-isosaccharinic acid. J. Chem. Therm. 138, 138 151–158. https://doi.org/10.1016/j.jct.2019.06.006.

Kopunec, R., Abudeab, F., Skrašková, S., 1998. Extraction of pertechnetate with tetraphenylphosphonium in the presence of various acids, salts and hydroxides. J. Radioanal. Nucl. Chem. 230 (1–2), 51–61. https://doi.org/10.1007/bf02387446.

Maset, E.R., Sidhu, S.H., Fisher, A., Heydon, A., Worsfold, P.J., Cartwright, A.J., Keith-Roach, M.J., 2006. Effect of organic co-contaminants on technetium and rhenium speciation and solubility under reducing conditions. Environ. Sci. Technol. 40 (17), 5472–5477. https://doi.org/10.1021/es061157f.

Neck, V., Kim, J., 2001. Solubility and hydrolysis of tetravalent actinides. Radiochim. Acta 89 (1), 1–16. https://doi.org/10.1524/ract.2001.89.1.001.

Pavasars, I., Hagberg, J., Borén, H., Allard, B., 2003. Alkaline degradation of cellulose: mechanisms and kinetics. Journal of Polymers and the Environment, Journal of Polymers and the Environment 11 (2), 39–47. https://doi.org/10.1023/A:1024267704794.

Rai, D., Kitamura, A., 2017. Thermodynamic equilibrium constants for important isosaccharinate reactions: a review. J. Chem. Therm. 114, 135–143. https://doi.org/10.1016/j.jct.2017.02.012.

Rai, D., Yui, M., Moore, D.A., Rao, L., 2009. Thermodynamic model for ThO₂(am) solubility in isosaccharinate solutions. J. Solut. Chem. 38 (12), 1573–1587. https://doi.org/10.1007/s10953-009-9470-8.

Rai, D., Yui, M., Moore, D.A., 2012. Isosaccharinate complexes of Fe(III). J. Solut. Chem. 41 (11), 1906–1921. https://doi.org/10.1007/s10953-012-9911-7.

Shannon, R.D., 1976. Revised effective ionic radii and systematic studies of interatomic distances in halides and chalcogenides. Acta Crystallogr. Sect. A Cryst. Phys. Diffr. Theor. Gen. Crystallogr. 32 (5), 751–767. https://doi.org/10.1107/S0567739476001551.

Tasi, A., Gaona, X., Fellhauer, D., Böttle, M., Rothe, J., Dardenne, K., Polly, R., Grivé, M., Colas, E., Bruno, J., 2018a. Thermodynamic description of the plutonium–α-d-isosaccharinic acid system I: solubility, complexation and redox behavior. Appl. Geochem. 98, 247–264.

Tasi, A., Gaona, X., Fellhauer, D., Böttle, M., Rothe, J., Dardenne, K., Polly, R., Grivé, M., Colas, E., Bruno, J., 2018b. Thermodynamic description of the plutonium–α–d–isosaccharinic acid system ii: formation of quaternary Ca(II)–Pu (IV)–OH–ISA complexes. Appl. Geochem. 98, 351–366. https://doi.org/10.1016/j.apgeochem.2018.06.014.

Tits, J., Wieland, E., Bradbury, M., 2005. The effect of isosaccharinic acid and gluconic acid on the retention of Eu(III), Am(III) and Th(IV) by calcite. Appl. Geochem. 20 (11), 2082–2096. https://doi.org/10.1016/j.apgeochem.2005.07.004.

Van Loon, L.R., Glaus, M.A., 1998. Experimental and Theoretical Studies on Alkaline Degradation of Cellulose and its Impact on the Sorption of Radionuclides. Paul Scherrer Institut, Villigen, Switzerland.

Vercammen, K., Glaus, M., Van Loon, L.R., 2001. Complexation of Th(IV) and Eu(III) by α-isosaccharinic acid under alkaline conditions. Radiochim. Acta 89 (6), 393–402. https://doi.org/10.1524/ract.2001.89.6.393.

Warwick, P., Evans, N., Hall, T., Vines, S., 2003. Complexation of Ni(II) by α-isosaccharinic acid and gluconic acid from pH 7 to pH 13. Radiochim. Acta 91 (4), 233–240. https://doi.org/10.1524/ract.91.4.233.19971.

Warwick, P., Evans, N., Hall, T., Vines, S., 2024. Stability constants of uranium(IV)-α-isosaccharinic acid and gluconic acid complexes. Radiochim. Acta 92 (12), 897–902. https://doi.org/10.1524/ract.92.12.897.55106.

Xia, Y., Hess, N.J., Felmy, A.R., 2006. Stability constants of technetium(IV) oxalate complexes as a function of ionic strength. Radiochim. Acta 94 (3), 137–141. https://doi.org/10.1524/ract.2006.94.3.137.

Yalçıntaş, E., Gaona, X., Scheinost, A.C., Kobayashi, T., Altmaier, M., Geckeis, H., 2015. Redox chemistry of Tc(VII)/Tc(IV) in dilute to concentrated NaCl and MgCl₂ solutions. Radiochim. Acta 103 (1), 57–72. https://doi.org/10.1515/ract-2014-2272.

Yalçıntaş, E., Gaona, X., Altmaier, M., Dardenne, K., Polly, R., Geckeis, H., 2016. Thermodynamic description of Tc(IV) solubility and hydrolysis in dilute to concentrated NaCl, MgCl₂ and CaCl₂ solutions. Dalton Trans. 45 (21), 8916–8936. https://doi.org/10.1039/C6DT00973E.